gators have compared the activation energy of the magnetic relaxation process with that derived from the dc conductivity data without mentioning the problems, which are involved in polycrystralline samples.

Comparing our results of the conductivity and the permeability measurements two activation energies W_b and W_L as derived from the electrical properties and two activation energies W_I and W_{III} as derived from the magnetic loss peak data are available, when leaving aside the activation energy W_{II} of the above-mentioned effect. It seems to be reasonable to compare only the activation energy W_b of the bulk material with the activation energies derived for the magnetic relaxation processes. Since the same values of the activation energy are found for W_b as well as for W_I these effects seem to be of the same origin. For example from Fig. 2 and Fig. 4 one can derive $W_b \approx 0.11$ eV and $W_I \approx 0.11$ eV for a specimen with 0.24 wt% Fe^{2+} ions, corresponding to 1.5×10^{20} ions $\times$ cm^{-3}. We assume that, particularly at high frequencies, the conductivity of the bulk material is due to an electron transfer between Fe^{3+} and Fe^{2+} ions on octahedral sites in a sublattice.[6] Basing upon the equality of W_b and W_I and by considering that the loss peak I is predominating, the same electron transfer seems to cause the magnetic relaxation I. Because of the absence of magnetic relaxations in samples of $BaFe_{12}^{3+}O_{19}$ without Fe^{2+} ions the relaxation III seems to be due to an electron transfer between Fe^{2+} and Fe^{3+} ions, too, but probably between other than octahedral sites.

The activation energy W_L which is related to the conductivity σ_L of the layers seems to be a value which is connected with the grain boundary barriers.[13]

ACKNOWLEDGMENTS

The author wishes to thank the Technology Department of this institute for the preparation of the samples. He is grateful to Professor H.P.J. Wijn for many stimulating discussions.

[13] J. Krausse, P. Dullenkopf, F. Haberey, and H. P. J. Wijn, Conference on Magnetic Oxides, Bucharest, 1968.

JOURNAL OF APPLIED PHYSICS VOLUME 40, NUMBER 7 JUNE 1969

Theory for the First-Order Spin-Wave Instability Threshold in Ferromagnetic Insulators of Ellipsoidal Shape with an Arbitrary Pumping Configuration*

CARL E. PATTON
Raytheon Research Division, Waltham, Massachusetts 02154
(Received 15 November 1968; in final form 27 January 1969)

The spin-wave instability theory of nonlinear effects in ferromagnetic insulators developed by Suhl for perpendicular pumping and by Schlömann for parallel pumping has been extended to include pumping with an arbitrary microwave field configuration. The theory is applicable to samples of ellipsoidal shape, magnetized to saturation along one principal axis, but not necessarily an axis of rotational symmetry as in the Suhl theory. The theory, in its present form, is quite versatile and applicable to a large variety of situations which are not accessible on the basis of the earlier calculations. Equations are developed specifically for first-order processes. Several examples are considered to demonstrate the versatility of the theory: (1) Perpendicular pumping with a linearly polarized microwave field; (2) oblique pumping with a linearly polarized field at an angle between 0° and 90° to the static field; (3) perpendicular pumping with a circularly polarized field rotating in the anti-Larmor sense.

INTRODUCTION

Although the spin-wave instability theory of nonlinear effects in ferromagnetic insulators developed by Suhl[1] and Schlömann *et al.*[2] is quite general in concept, the specific calculations were done only for restricted pumping configurations and sample shapes. Pumping configurations were restricted to linearly polarized microwave fields along the static field direction (parallel pumping) or circularly polarized fields perpendicular to the static field direction with the proper sense of rotation to excite ferromagnetic resonance (perpendicular pumping). The results are applicable to samples of ellipsoidal shape magnetized to saturation along a principal axis. For perpendicular pumping the saturation direction must also be an axis of rotational symmetry. The theory has been extended to include: (1) samples of ellipsoidal shape magnetized to saturation by an applied static field H_0 along a principal axis, not necessarily an axis of rotational symmetry; (2) an arbitrary configuration for the microwave field. A general expression for the first-order instability threshold field as a function of spin-wave propagation direction, statis field, sample shape, and pumping configuration is obtained. Results are presented for several interesting special cases, primarily to illustrate the versatility of the theory. Three cases are considered: (1) perpendicular pumping with a linearly polarized

* This work was supported by the Advanced Research Projects Agency of the Department of Defense and was monitored by Rome Air Development Center under Contr. No. F 30602-68-C-0005.

[1] H. Suhl, J. Phys. Chem. Solids **1**, 209 (1957).

[2] See E. Schlömann, J. J. Green, and U. Milano, J. Appl. Phys. **31**, 386S (1960).

Downloaded 04 Mar 2004 to 129.82.140.198. Redistribution subject to AIP license or copyright, see http://jap.aip.org/jap/copyright.jsp

microwave excitation; (2) perpendicular pumping with a circularly polarized microwave field rotating in the anti-Larmor sense (opposite to that required for ferromagnetic resonance), and (3) pumping with a linearly polarized microwave field at an arbitrary angle to the saturation direction. Similar results for these special cases and an infinite magnetic medium were reported by Kitaev *et al.*[3] The special case of oblique pumping was also examined by Stern[4] and Green *et al.*[5]

SPIN-WAVE EQUATION OF MOTION

The equation of motion for the spin-wave amplitude α_k, first obtained by Suhl[1] and discussed by Schlömann,[6] is the basis for the present extension of the theory to the general case. The approach and the mathematics closely follow the discussion in Ref. 6. Consider the undamped equation of motion for the magnetization $\mathbf{M}(\mathbf{r})$ in terms of a unit vector $\boldsymbol{\alpha}(\mathbf{r})=\mathbf{M}(\mathbf{r})/M$:

$$d\boldsymbol{\alpha}(\mathbf{r})/dt=-\gamma\boldsymbol{\alpha}(\mathbf{r})\times\mathbf{H}(\mathbf{r}), \tag{1}$$

where γ is the gyromagnetic ratio, assumed positive for electrons, $4\pi M$ is the saturation induction and $\mathbf{H}(\mathbf{r})$ is the total internal magnetic field. The internal field consists of four parts, the static external field $\mathbf{H}_0$, the external microwave field $\mathbf{h}_0$, an effective field due to exchange $\mathbf{H}_{ex}(\mathbf{r})$, and an effective field due to dipolar interactions $\mathbf{H}_{\text{dip}}(\mathbf{r})$. All fields except $\mathbf{H}_0$ are assumed to vary as $\exp(i\omega t)$ where ω is the angular excitation frequency. By expanding the $\alpha(r)$ in a Fourier series

$$\boldsymbol{\alpha}(\mathbf{r})=\sum_{k}\boldsymbol{\alpha}_k\exp(i\mathbf{k}\cdot\mathbf{r}), \tag{2}$$

assuming that $\mathbf{H}_0$ and $\mathbf{h}_0$ are uniform over the sample volume, selecting the coordinate axes to be along the principal axes of the saturated ellipsoidal sample with $\mathbf{H}_0$ in the z direction, and assuming that $M_z\approx M$ is satisfied, the equation of motion for $\boldsymbol{\alpha}_k$ can be obtained. The vector $\mathbf{k}$ is the propagation constant or wave vector for the spin wave, and the $\boldsymbol{\alpha}_k$ are spin-wave amplitudes defined by Eq. (2). Following Schlömann,[6] the external fields may be expressed in terms of internal fields,

$$H=H_0-4\pi MN_z \tag{3a}$$

and

$$h_{x,y}=h_0{}^{x,y}-4\pi MN_{x,y}\alpha_0{}^{x,y}, \tag{3b}$$

where N_x, N_y, and N_z are the sample demagnetizing factors. The result can be expressed in terms of complex variables

$$\alpha_k=\alpha_k{}^x+i\alpha_k{}^y,$$
$$k_T=k_x+ik_y, \tag{4a}$$

and

$$h=h_x+ih_y. \tag{4b}$$

The equation of motion is

$$\dot{\alpha}_k=i\gamma\{[H+h_0{}^z+4\pi MN_z(1-\alpha_0{}^2)]\alpha_k-\alpha_k{}^z h+D\sum_{k'}(k')^2(\alpha_{k'}a_{k-k'}{}^z-\alpha_{k'}{}^z\alpha_{k-k'})+4\pi M\sum_{k'\neq 0}(\mathbf{k}'\cdot\boldsymbol{\alpha}_{k'})[(k_T'\alpha_{k-k'}{}^z-k_z'\alpha_{k-k'})/(k')^2]\} \tag{5}$$

with

$$\alpha_k{}^z=\delta_{k0}-\tfrac{1}{2}\sum_{k'}\alpha_{k'}\alpha_{k-k'}{}^*, \tag{6}$$

where D is a phenomenological exchange parameter defined by $\mathbf{H}_{ex}(\mathbf{r})=D\nabla^2\boldsymbol{\alpha}(\mathbf{r})$ and δ_{k0} is the Kronecker delta function.

In a conventional low-power microwave experiment, only the uniform mode is excited to a large amplitude and the α_k, other than for $\mathbf{k}=0$, are negligibly excited. Therefore, only terms to first order in the α_k with $\mathbf{k}\neq 0$ need be considered. The equation of motion for α_k with $\mathbf{k}\neq 0$ is

$$\dot{\alpha}_k=i\{(A_k+C_k)\alpha_k+[B_k\exp(2i\phi_k)+D_k]\alpha_{-k}{}^*\}+i\gamma h_0{}^z\alpha_k, \tag{7}$$

where

$$A_k=\gamma H+\gamma Dk^2+\tfrac{1}{2}\omega_m\sin^2\theta_k, \tag{8a}$$

$$B_k=\tfrac{1}{2}\omega_m\sin^2\theta_k, \tag{8b}$$

$$C_k=-\tfrac{1}{2}\omega_m\cos\theta_k\sin\theta_k[\exp(-i\phi_k)\alpha_0+\exp(i\phi_k)\alpha_0{}^*]+\tfrac{1}{4}\omega_m[2N_z+(3\cos^2\theta_k-1)]\,|\,\alpha_0\,|^2+\tfrac{1}{2}\gamma h a_0{}^*, \tag{8c}$$

and

$$D_k=\tfrac{1}{2}\gamma Dk^2\alpha_0{}^2-\omega_m\cos\theta_k\sin\theta_k\exp(i\phi_k)\alpha_0+\tfrac{1}{4}\omega_m(2\cos^2\theta_k\alpha_0{}^2-\sin^2\theta_k\exp(2i\phi_k)\,|\,\alpha_0\,|^2)+\tfrac{1}{2}\gamma h\alpha_0. \tag{8d}$$

In Eqs. (8a)–(8d) ω_m is equal to $\gamma 4\pi M$, θ_k is the angle between the spin-wave wave vector $\mathbf{k}$ and the saturation direction, and ϕ_k is the angle between the projection of $\mathbf{k}$ on the x–y plane perpendicular to the saturation direction and the x axis. For $\mathbf{h}_0=0$, α_0 vanishes and C_k and D_k are both zero. The remaining A_k and B_k terms can be diagonalized by a linear Holstein–Primakoff transformation

$$b_k=\lambda_k\alpha_k+\mu_k\alpha_{-k}{}^*, \tag{9}$$

with

$$\lambda_k=\cosh(\psi_k/2), \tag{10a}$$

and

$$\mu_k=\sinh(\psi_k/2)\exp(2i\phi_k), \tag{10b}$$

where

$$\cosh\psi_k=A_k/\omega_k, \tag{11a}$$

$$\sinh\psi_k=B_k/\omega_k, \tag{11b}$$

and

$$\omega_k=(A_k{}^2-B_k{}^2)^{1/2}=[(\gamma H+\gamma Dk^2)(\gamma H+\gamma Dk^2+\omega_m\sin^2\theta_k)]^{1/2}. \tag{11c}$$

Expressed in terms of the b_k, the equation of motion

---

[3] L. V. Kitaev, A. A. Goncharova, and G. I. Katamaran, Fiz. Tverd. Tela **9**, 330 (1967) [Sov. Phys.—Solid State **9**, 246 (1967)].

[4] E. Stern, G-MTT International Microwave Symposium, Boston, 1967, IEEE Cat. No. 17C66, p. 103.

[5] J. J. Green, E. Stern, and C. E. Patton, J. Appl. Phys. **40**, 172 (1969).

[6] E. Schlömann, Raytheon Tech. Rep. R-48 (1959). See also E. Schlömann and R. I. Joseph, Raytheon Tech. Rep. R-68 (1968) [to be published in J. Smit, *Magnetic Properties of Materials* (McGraw-Hill Book Co., New York)].

Downloaded 04 Mar 2004 to 129.82.140.198. Redistribution subject to AIP license or copyright, see http://jap.aip.org/jap/copyright.jsp

becomes

$$\dot{b}_k = i\{\omega_k b_k + (F_k + \gamma h_0{}^z A_k/\omega_k) b_k + [G_k - \gamma h_0{}^z B_k \exp(2i\phi_k)/\omega_k] b_k{}^*\}. \quad (12)$$

The F_k and G_k have been calculated in Ref. 6, and are given by

$$F_k = C_k\lambda_k{}^2 + C_k{}^* \mid \mu_k \mid{}^2 + D_k\lambda_k\mu_k{}^* - D_k{}^*\lambda_k\mu_k, \quad (13)$$

and

$$G_k = D_k\lambda_k{}^2 + D_k{}^*\mu_k{}^2 - (C_k + C_k{}^*)\lambda_k\mu_k = [\exp(2i\phi_k)/2\omega_k][D_k(A_k+\omega_k)\exp(-2i\phi_k) + D_k{}^*(A_k-\omega_k)\exp(2i\phi_k) - (C_k+C_k{}^*)B_k]. \quad (14)$$

The equation of motion in Eq. (12) contains a contribution due to the transverse components of $\mathbf{h}_0$ in the F_k and G_k terms, and a contribution due to the parallel component of $\mathbf{h}_0$ in the $h_0{}^z$ terms.

GENERAL FIRST-ORDER INSTABILITY THRESHOLD

From Eqs. (12) and (14), the threshold fields can be calculated in a straightforward manner as described in Ref. 6. The $G_k - \gamma h_0{}^z B_k \exp(2i\phi_k)/\omega_k$ coupling term leads to an unstable growth of the b_k with time for sufficiently high microwave power levels. The $F_k + \gamma h_0{}^z A_k/\omega_k$ term leads only to a slight modulation and shift of the spin-wave frequency and can be neglected. For convenience, let

$$\tilde{G}_k = G_k - \gamma h_0{}^z B_k \exp(2i\phi_k)/\omega_k, \quad (15)$$

consider an equation of motion of the form

$$b_k = i(\omega_k b_k + \tilde{G}_k b_{-k}{}^*), \quad (16)$$

and introduce energy dissipation by replacing ω_k by $\Omega_k = \omega_k + i\eta_k$ where η_k is the relaxation rate for the b_k. This relaxation rate is related to the spin-wave linewidth ΔH_k by $\Delta H_k = 2\eta_k/\gamma$. The $\tilde{G}_k$ can be expressed as

$$\tilde{G}_k = \sum_{n=-2}^{n=+2} \tilde{G}_k{}^{(n)} \exp(in\omega t), \quad (17)$$

and the first-order instability can be evaluated by considering only the $n=1$ term of Eq. (17), that part of G_k which varies as $\exp(i\omega t)$. Similarly, the second-order instability is obtained by considering the $n=2$ term, although this case will not be examined here. Considering the $n=1$ term only, the equation of motion becomes

$$b_k = i\{\Omega_k b_k + \tilde{G}_k{}^{(1)} \exp(i\omega t) b_{-k}{}^*\}. \quad (18)$$

It is convenient to rewrite this equation in terms of a new variable $b_{k0}(t)$ defined by

$$b_k = b_{k0}(t) \exp(i\omega t/2), \quad (19)$$

and examine the conditions under which a stationary solution for the b_{k0} is permitted. By combining the differential equations for b_{k0} and $b_{-k0}{}^*$ which result from Eq. (18) and (19), one obtains a second-order differential equation,

$$\left\{\frac{d^2}{dt^2} + 2\eta_k \frac{d}{dt} + \left[\left(\omega_k - \frac{\omega}{2}\right)^2 + \eta_k{}^2 - \mid \tilde{G}_k{}^{(1)} \mid{}^2\right]\right\} b_{k0} = 0, \quad (20)$$

which has a solution $b_{k0} \propto \exp(\kappa t)$ where

$$\kappa = \eta_k \pm \{\mid \tilde{G}_k{}^{(1)} \mid{}^2 - [\omega_k - (\omega/2)]^2\}^{1/2}. \quad (21)$$

The stationary solution corresponds to $\kappa = 0$. The smallest value of $\mid \tilde{G}_k{}^{(1)} \mid$ for which this solution is permitted occurs when the spin-wave frequency ω_k is equal to one half the excitation frequency ω and $\mid \tilde{G}_k{}^{(1)} \mid = \eta_k$ is satisfied. This condition on $\tilde{G}_k{}^{(1)}$ determines the instability threshold amplitude for the state $(\omega/2, k)$. Larger amplitudes result in a positive κ and an exponential increase in b_{k0} with time.

The problem reduces to the extraction of $\tilde{G}_k{}^{(1)}$ from Eqs. (8), (14), (15), and (17). To obtain $\tilde{G}_k{}^{(1)}$ it is necessary to consider the explicit time dependence of $\mathbf{h}_0$ and the resultant uniform precession amplitude α_0. Let h_0 be given by

$$h_0{}^x = h_0 a_x \cos(\omega t + \delta_x), \quad (22a)$$

$$h_0{}^y = h_0 a_y \cos(\omega t + \delta_y), \quad (22b)$$

and

$$h_0{}^z = h_0 a_z \cos(\omega t). \quad (22c)$$

Equations (22a)–(22c) can be used to describe most experimentally attainable drive configurations. For example, setting δ_x and δ_y to zero and requiring that $a_x{}^2 + a_y{}^2 + a_z{}^2$ equal unity corresponds to linearly polarized excitation making an angle $\Psi = \cos^{-1} a_z$ with respect to the z direction and an angle $\Phi = \cos^{-1} a_x$ with respect to the x direction. With the abbreviations

$$X = \gamma(H + 4\pi M N_x), \quad (23a)$$

and

$$Y = \gamma(H + 4\pi M N_y), \quad (23b)$$

the complex uniform precession amplitude α_0 can be calculated from Eqs. (1), (2), (4), (22), and (23) to be

$$\alpha_0 = (\gamma h_0/2)[q_L \exp(i\omega t) + q_A \exp(-i\omega t)], \quad (24)$$

where

$$q_L = \frac{(\omega+Y)a_x \exp(i\delta_x) + i(\omega+X)a_y \exp(i\delta_y)}{XY - \omega^2}$$

and

$$q_A = -\frac{(\omega-Y)a_x \exp(-i\delta_x) + i(\omega-X)a_y \exp(-i\delta_y)}{XY - \omega^2}.$$

Damping of the uniform precession may be taken into account by replacing X and Y by $\Omega_{0x} = X + i\eta_0$ and $\Omega_{0y} = Y + i\eta_0$, respectively. As long as $\mid \omega - \omega_0 \mid \gg \eta_0$ is satisfied, damping may be neglected completely without significantly modifying the results. Near resonance, however, the uniform-mode relaxation rate η_0 must be taken into account.

The contributions to $\tilde{G}_k{}^{(1)}$ are determined only by the explicit time dependences of $h_0{}^z$ and G_k. From Eqs. (15) and (22), the $h_0{}^z$ contribution is simply

Downloaded 04 Mar 2004 to 129.82.140.198. Redistribution subject to AIP license or copyright, see http://jap.aip.org/jap/copyright.jsp

$-(\omega_m/\omega)(\gamma h_0/2)\sin^2\theta_k a_z \exp(2i\phi_k)$. The G_k contribution is determined by Eqs. (8), (14), (22), and (24). The A_k and B_k have no explicit time dependence. The only terms in C_k, D_k, and their complex conjugates which vary as $\exp(i\omega t)$ are those which contain α_0 or α_0^* to first order and do not contain h_0 explicitly. After collecting all terms in $\tilde{G}_k$ which vary as $\exp(i\omega t)$ the result is

$$\tilde{G}_k^{(1)} = -(\omega_m/\omega)(\gamma h_0/2) \times (\sin\theta_k \cos\theta_k \{q_L[f(\theta_k)+(\omega/2)]\exp(-i\phi_k) + q_A^*[f(\theta_k)-(\omega/2)]\exp(i\phi_k)\} + \sin^2\theta_k a_z). \quad (25)$$

In the above

$$f(\theta_k) = \tfrac{1}{2}[(\omega_m^2 \sin^4\theta_k + \omega^2)^{1/2} - \omega_m \sin^2\theta_k], \quad (26)$$

and $f(\theta_k)$ is equal to $\gamma H + \gamma D k^2$ in the dispersion relation of Eq. (11c). The instability-threshold field amplitude for spin-wave state $(\omega_k = \omega/2, \theta_k, \phi_k)$ is simply the value of h_0 for which $|G_k^{(1)}| = \gamma \Delta H_k/2$ is satisfied. Let W be defined by

$$\tilde{G}_k^{(1)} = -(\omega_m/\omega)(\gamma h_0/2)\exp(2i\phi_k) W. \quad (27)$$

$$W = \sin\theta_k \cos\theta_k \{q_L[f(\theta_k)+(\omega/2)]\exp(-i\phi_k) + q_A^*[f(\theta_k)-(\omega/2)]\exp(i\phi_k) + \sin^2\theta_k a_z\}. \quad (28)$$

The threshold h_c is given by

$$h_c = (\omega/\omega_m)(\Delta H_k/|W|). \quad (29)$$

First-order processes are restricted to external field values for which spin waves with $\omega_k = \omega/2$ are allowed. From Eq. (11c), this condition is equivalent to the requirement $\omega/2 > \gamma H$. As γH approaches $\omega/2$, θ_k approaches zero and the sin θ_k factor in W causes h_c to diverge.

The experimentally observed threshold for a first-order instability should correspond to the minimum value of h_c with respect to k for a given sample geometry, microwave field configuration, and applied static field. This theoretical minimum can be obtained by minimizing $|W|^{-1}$ with respect to θ_k and ϕ_k subject to the condition that the value of k at the minimum be real. This condition is equivalent to the requirement

$$f(\theta_k) - \gamma H \geq 0. \quad (30)$$

Let $\theta_k^{(\min)}$ and $\phi_k^{(\min)}$ be the values of θ_k and ϕ_k which minimize $|W|^{-1}$. If $\theta_k^{(\min)}$ does not satisfy the inequality of Eq. (30), the $\theta_k^{(\min)}$ which actually corresponds to the instability threshold is given by the θ_k solution to $f(\theta_k) - \gamma H = 0$ and k is zero.

$$h_{\text{crit}} = \frac{\omega}{\omega_m} \frac{\Delta H_k}{|W(\theta_k^{(\min)}, \phi_k^{(\min)})|}, \quad (31)$$

is the expected first-order instability threshold field for a given sample geometry, microwave field configuration, and static field.

In the above analysis, a first-order spin-wave instability threshold expression has been obtained for samples of ellipsoidal shape magnetized to saturation along a major axis and an arbitrary microwave pumping field configuration. No assumptions were made concerning sample symmetry, other than the ellipsoidal shape, or microwave field geometry, except that all fields were assumed uniform over the sample volume. Insofar as most of the analysis is quite similar to that previously reported by Suhl[1] and Schlömann,[6] it is important to briefly summarize the specific differences between this and the earlier calculations. The first difference is the inclusion of both a parallel component h_0^z and transverse components, h_0^x and h_0^y, of the external microwave field in the initial equation of motion given by Eq. (5). By considering only terms to first order in the α_k due to both parallel and transverse field components in the equation of motion and applying a linear Holstein–Primakoff transformation to these terms, the coupling coefficient in the equation of motion which leads to instability, expressed by $\tilde{G}_k$ of Eq. (16), is obtained for a general microwave field configuration. The second difference rests in the expression for the uniform precession amplitude α_0 which was used to evalute the coupling coefficient associated with the transverse components of h_0. By utilizing the general expression for α_0 given by Eq. (24), which is valid for an arbitrary transverse microwave field polarization and different transverse demagnetizing factors, the requirements on sample symmetry and the transverse pump polarization are eliminated. These two changes constitute the major differences between the present calculation and the earlier theories. For simplicity, the discussion has been limited to first-order instability processes. Second-order processes and the steady-state behavior above threshold have not been considered explicitly. From the general expression for $\tilde{G}_k$ of Eq. (15), the threshold for second-order processes with $\omega_k = \omega$ and $n = 2$ can be easily evaluated in a manner analogous to that presented here. Steady-state behavior can be calculated by including higher-order terms in Eq. (9).

DISCUSSION FOR SPECIAL CASES

The above refinements in the theory result in several modifications of the earlier predictions and extend the applicability of the theory to more general geometries and microwave field configurations. It is illustrative to consider several special cases which demonstrate new or modified results of the extended theory. Three specific situations for first-order processes will be considered: (1) perpendicular pumping with linearly polarized microwave excitation; (2) perpendicular pumping with circularly polarized drive rotating in the anti-Larmor sense; (3) oblique pumping with linearly polarized drive. In case (1), the contribution of the anti-Larmor rotating component of the linearly polarized pump field to h_{crit} will be demonstrated and the effect of sample geometry on the threshold will also be considered. In case (2), the threshold for anti-Larmor pumping will be calculated and compared with h_{crit} for Larmor pumping. In case (3), the dependence of

Downloaded 04 Mar 2004 to 129.82.140.198. Redistribution subject to AIP license or copyright, see http://jap.aip.org/jap/copyright.jsp

h_{crit} on the angle between the polarization axis for a linear polarized pump field and the static field direction will be demonstrated. In all cases the dependence of ΔH_k on $\mathbf{k}$ will be neglected in the minimization procedure [as it was in the discussion leading to Eq. (31)]. Actual h_{crit} curves would be slightly modified because of this $\mathbf{k}$ dependence. It is also assumed that $|\omega-\omega_0| \gg \eta_0$ is always satisfied so that η_0 need not be taken into account. This assumption excludes the possibility of a first-order instability at resonance ($\omega=\omega_0$). Such coincidence effects have been discussed at length.[6] The results to follow apply specifically to situations where first-order processes are allowed only for fields less than that required for resonance so that $\omega_0<\omega$ is satisfied.

Case (1). For perpendicular pumping with a linearly polarized microwave field in the x direction, δ_x, a_y, and a_z in Eq. (22) are zero, a_x is equal to unity, and the uniform precession amplitude is given by Eq. (24) with

$$q_L=(Y+\omega)/(XY-\omega^2), \tag{32a}$$

and

$$q_A=(Y-\omega)/(XY-\omega^2). \tag{32b}$$

With q_L and q_A from Eqs. (32a) and (32b), W in Eq. (28) simplifies to

$$W=\frac{\sin\theta_k\cos\theta_k}{\omega^2-XY}\{(Y+\omega)[f(\theta_k)+(\omega/2)] \times\exp(-i\phi_k)+(Y-\omega)[f(\theta_k)-(\omega/2)]\exp(i\phi_k)\}. \tag{33}$$

The ϕ_k spin-wave angle determines the relative phases

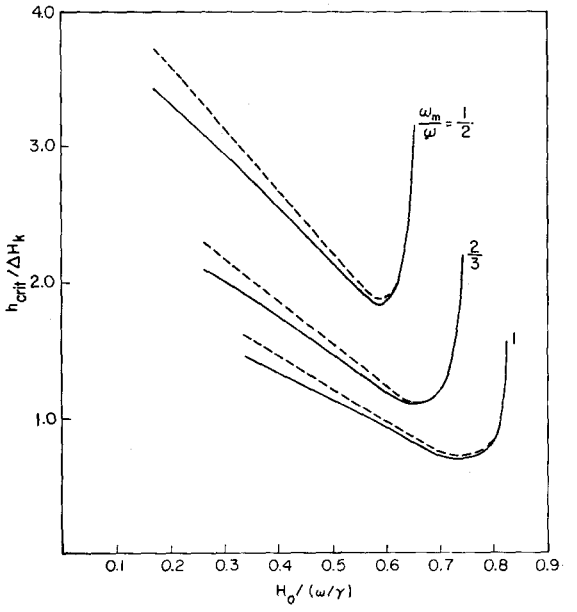

FIG. 1. First-order spin-wave instability threshold field h_{crit} normalized to the spin-wave linewidth ΔH_k as a function of the static external field H_0 normalized to ω/γ, the angular excitation frequency divided by the gryomagnetic ratio. Curves were obtained for spherical samples and a linearly polarized microwave excitation, with ω_m/ω ($\omega_m=\gamma 4\pi M$ is the saturation induction) as a parameter. The dotted curves neglect the contribution of the anti-Larmor component of the microwave field to h_{crit}.

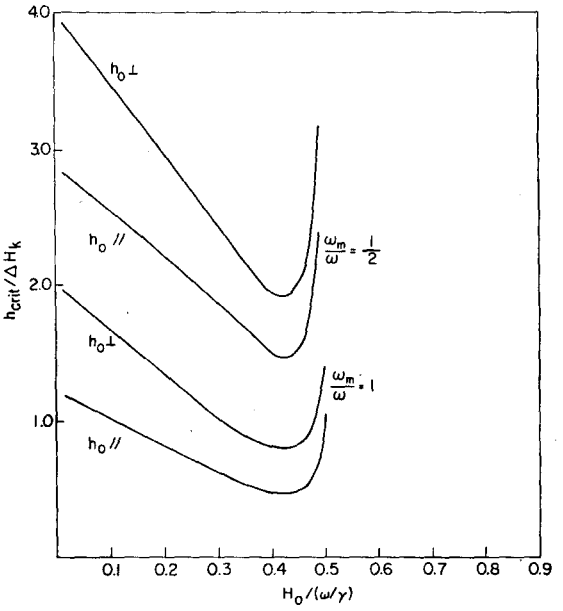

FIG. 2. Normalized threshold h_{crit} as a function of the normalized field H_0. Curves are shown for thin disk-shaped samples with an in-plane demagnetizing factor of zero and linearly polarized microwave excitation parallel to (h_0 ||) or perpendicular to ($h_0\perp$) the slab plane. The slab was assumed to be magnetized to saturation in its plane and perpendicular to the microwave field direction. Sets of curves are shown for $\omega_m/\omega=\frac{1}{2}$ and $\omega_m/\omega=1$.

of the two complex terms in the curly brackets of Eq. (33). The magnitude of W is maximized and the threshold h_c is minimized for $\phi_k=\phi_k^{(\min)}$ such that the phases of these two terms are equal.

$$|W(\theta_k,\phi_k^{(\min)})|=\frac{\sin\theta_k\cos\theta_k}{|\omega^2-XY|} \times\{(\omega+Y)[(\omega/2)+f(\theta_k)]+|\omega-Y|[(\omega/2)-f(\theta_k)]\}. \tag{34}$$

The minimization of $|W(\theta_k,\phi_k)^{(\min)}|^{-1}$ and h_c with respect to θ_k determines the threshold and h_{crit} is given by

$$h_{crit}=\frac{\omega}{\omega_m}\frac{\Delta H_k|\omega^2-XY|}{\sin\theta_k^{(\min)}\cos\theta_k^{(\min)}} \times\{(\omega+Y)[(\omega/2)-f(\theta_k^{(\min)})] +|\omega-Y|[(\omega/2)-f(\theta_k^{(\min)})]\}^{-1}.$$

The value for $\theta_k^{(\min)}$ is a complicated function of the sample shape, frequency, magnetization, and applied field. The value of $\phi_k^{(\min)}$, however, is determined only by the relative signs of the real terms in Eq. (33). With $f(\theta_k)$ as defined by Eq. (26), the expression $[f(\theta_k)-\omega/2]$ is always negative. If $(Y-\omega)$ is also negative, $\phi_k^{(\min)}$ is 0 or π. If $(Y-\omega)$ is positive, $\phi_k^{(\min)}$ is $\pm\pi/2$. The static internal field value below which $\phi_k^{(\min)}$ is 0 or π and above which $\phi_k^{(\min)}$ is $\pm\pi/2$ is determined by

$$Y-\omega=\gamma H+\gamma 4\pi M N_y-\omega=0. \tag{36}$$

For first-order processes, the static internal field H is

Downloaded 04 Mar 2004 to 129.82.140.198. Redistribution subject to AIP license or copyright, see http://jap.aip.org/jap/copyright.jsp

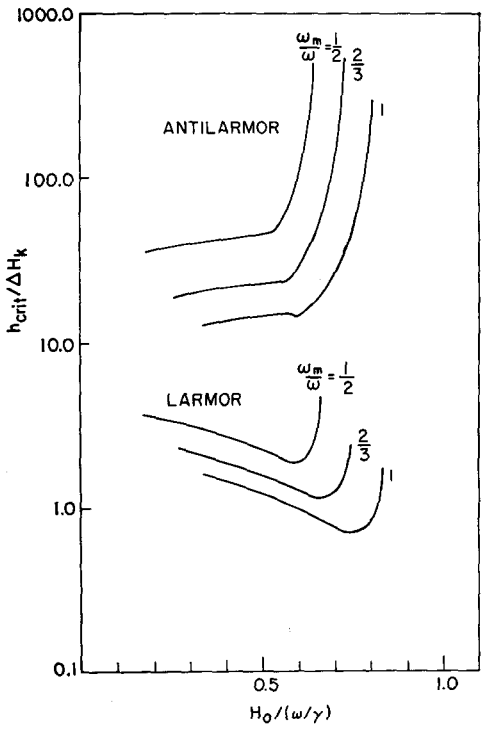

FIG. 3. Normalized threshold h_{crit} as a function of the normalized field H_0. Curves were calculated for spherical samples and a circularly polarized microwave excitation perpendicular to the static field direction, with ω_m/ω as a parameter. Results are shown for a Larmor excitation, rotating in the proper sense to excite ferromagnetic resonance, and an anti-Larmor excitation, rotating in the opposite sense.

constrained by the requirement $H<\omega/2\gamma$. The ϕ_k transition field is less than $\omega/2\gamma$ only if the N_y demagnetizing factor is greater than $\omega/2\omega_m$.

Equation (35) gives the instability threshold field expected for transverse pumping in a saturated ferromagnetic ellipsoid with a linearly polarized microwave field along a principal axis in the x direction and the static field along a principal axis in the z direction. The $(\omega+Y)$ and $(\omega-Y)$ terms in the numerator of Eq. (34) are due to the Larmor and anti-Larmor components of the linearly polarized field, respectively. Previously, the usual procedure for obtaining h_{crit} for a linearly polarized transverse pump field has been to apply the Suhl theory to the Larmor rotating component of the field and neglect the anti-Larmor component. Such a procedure would result in Eq. (34) with the second term in the curly brackets omitted. Results for spherical samples are shown in Fig. 1. Normalized curves of $h_{crit}/\Delta H_k$ are shown as a function of applied field H_0 normalized to (ω/γ) with ω_m/ω as a parameter. The solid curves correspond to h_{crit} when the anti-Larmor contribution is included and the dotted curves were calculated neglecting this contribution. These results show that the anti-Larmor term has a noticeable effect on h_{crit}. The threshold is smaller than the Suhl value and is not linear in H_0 on the low-field side of the minimum. The reduction is due to the anti-Larmor term in Eq. (35). The nonlinear behavior results from a field-dependent $\theta_k^{(min)}$.

Perpendicular pumping thresholds for samples which lack rotational symmetry about the field axis can be quite different from those obtained by using the Suhl theory with an average transverse demagnetizing factor. To demonstrate this point, curves of $h_{crit}/\Delta H_k$ vs $H_0/(\omega/\gamma)$ are shown in Fig. 2 for planar samples magnetized in their plane. Two cases were considered, h_0 parallel to the plane of the slab and h_0 perpendicular to the plane of the slab. In-plane demagnetizing factors of zero were assumed. For h_0 perpendicular to the plane of the slab, the threshold amplitude is significantly higher than for h_0 in the plane. This result can be explained by considering the effect of geometry on the uniform precession amplitude α_0, which is the important parameter in determining the threshold for perpendicular pumping. For a parallel h_0, Y is given by $Y=\gamma H+\omega_m$. For a normal h_0, $Y=\gamma H$ is satisfied. From Eq. (32a), q_L is larger for h_0 parallel to the plane of the slab than for h_0 normal to the slab. Consequently, a normal h_0 is less efficient in pumping the uniform precession than an in-plane h_0 and the h_{crit} for a microwave field perpendicular to the slab is higher. Such differences are not accessible when rotational symmetry is assumed. All transverse directions are then equivalent.

Case (2). The instability threshold for perpendicular

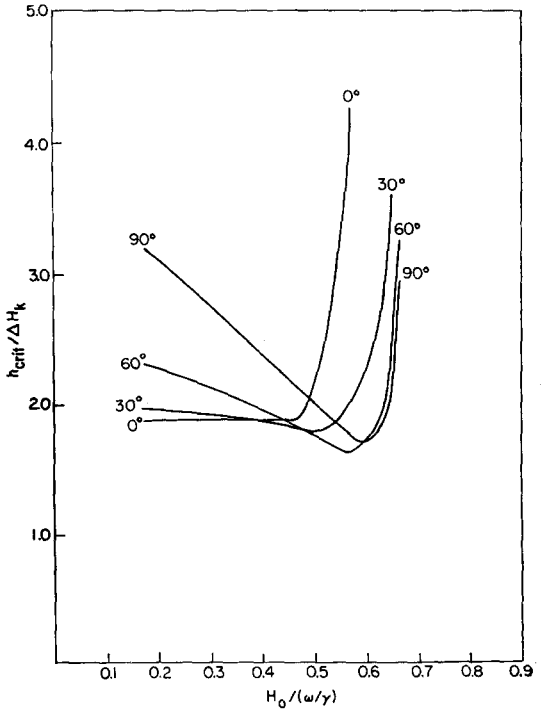

FIG. 4. Normalized threshold field h_{crit} as a function of the normalized field H_0. Curves were calculated for spherical samples and a linearly polariaed microwave field at angles of 0°, 30°, 60°, and 90° to the static field direction. The curves were obtained with ω_m/ω equal to 0.54, which is appropriate for YIG at 9.2 GHz.

Downloaded 04 Mar 2004 to 129.82.140.198. Redistribution subject to AIP license or copyright, see http://jap.aip.org/jap/copyright.jsp

pumping with a circularly polarized microwave field rotating in an anti-Larmor sense can be obtained by omitting the $(\omega+Y)$ term in Eq. (33) and multiplying the expression by two. The factor of two compensates for the factor of one half between the amplitude of a linearly polarized field and the amplitude of its Larmor or anti-Larmor rotating components. For comparison, the instability threshold for Larmor pumping may be evaluated by setting the $(\omega-Y)$ term in Eq. (33) to zero, as in the Suhl theory, and including the factor of two. Theoretical curves for both cases are shown in Fig. 3. The upper set of curves correspond to anti-Larmor pumping and the lower set to Larmor pumping. The curves were calculated for spherical samples. The results in Fig. 3 illustrate two important points concerning anti-Larmor pumping. (1) The threshold is significantly higher than for Larmor pumping. (Note that the h_{crit} axis is logarithmic.) (2) The threshold does not, in general, exhibit the usual minimum which is characteristic of Larmor pumping, although the anti-Larmor curve does exhibit a small, local minimum for large ω_m/ω.

Case (3). Finally, consider oblique pumping with a linearly polarized microwave field making an angle Ψ with the direction of the static external field and polarized in the $x-z$ plane. This field corresponds to $\alpha_y=0$, $\delta_z=0$, $\alpha_x=\sin\Psi$, and $\alpha_z=\cos\Psi$. Also assume, for simplicity, that the static field is along an axis of rotational symmetry so that X and Y are both equal to the natural uniform precession frequency ω_0. With these assumptions,

$$q_L=\sin\Psi/(\omega_0-\omega), \tag{37a}$$

and

$$q_A=\sin\Psi/(\omega_0+\omega). \tag{37b}$$

For this situation, W in Eq. (28) simplifies to

$$W=\sin\theta_k\cos\theta_k\left(\frac{\sin\Psi[f(\theta_k)+(\omega/2)]}{\omega_0-\omega}\exp(-i\phi_k)\right.$$
$$\left.+\frac{\sin\Psi[f(\theta_k)-(\omega/2)]}{\omega_0+\omega}\exp(i\phi_k)\right)+\sin^2\theta_k\alpha_z. \tag{38}$$

As pointed out previously, $f(\theta_k)-\omega/2$ is negative. The requirement $\omega_0<\omega$ has been assumed so that the coefficients of the $\exp(\pm i\phi_k)$ terms in the curly brackets of Eq. (38) are both negative. Phases are matched for all terms only for $\phi_k=\pi$ so that $|W|$ is maximized and h_c minimized with respect to ϕ_k at $\phi_k^{(\min)}=\pi$. This result is strictly valid only if the damping of the uniform precession is neglected. If ω_0 is assigned an imaginary part η_0 corresponding to the uniform precession relaxation rate as described in the last section, the phases of the terms in the curly brackets of Eq. (38) are modified. The change is small for small damping.

If the uniform precession damping is neglected, $\phi_k^{(\min)}$ is exactly π and $|W|$ is given by

$$|W(\theta_k,\phi_k^{(\min)})|=\sin\theta_k\{[\cos\theta_k\sin\Psi/(\omega^2-\omega_0^2)]$$
$$\times[2\omega_0 f(\theta_k)+\omega^2]+\cos\Psi\sin\theta_k\}. \tag{39}$$

The threshold h_{crit} is then obtained by minimizing $|W|^{-1}$ with respect to θ_k as discussed above. In Fig. 4, normalized curves of $h_{\text{crit}}/\Delta H_k$ as a function of $H_0/(\omega/\gamma)$ are shown with Ψ as a parameter. Spherical sample shape and $\omega_m/\omega=0.54$ corresponding to yttrium iron garnet at 9.2 GHz were assumed. The curve for $\Psi=0°$ corresponds to parallel pumping and the $\Psi=90°$ curve corresponds to perpendicular pumping. The curves illustrate the dependence of $h_{\text{crit}}/\Delta H_k$ on pumping angle. At low field, $h_{\text{crit}}/\Delta H_k$ increases with Ψ and is most sensitive to angles near $\Psi=90°$. At high field, $h_{\text{crit}}/\Delta H_k$ decreases with Ψ and is most sensitive to angles near $\Psi=0°$. The threshold field minimum moves to higher static field with increasing Ψ.

SUMMARY AND CONCLUSION

Spin-wave instability theory has been extended to include pumping with an arbitrary microwave field configuration and ellipsoidal samples magnetized along a principal axis which is not necessarily an axis of rotational symmetry. The calculations have been carried out explicitly for the first-order instability threshold. Several special cases have been considered to demonstrate the versatility of the theory in analyzing situations previously inaccessible on the basis of the original theoretical treatments. Sample geometry and the pump configuration have a strong influence on the instability threshold amplitude.

ACKNOWLEDGMENTS

The author is indebted to E. Schlömann for helpful discussions concerning spin-wave instability theory and to Mrs. B. Matsinger for assistance with the numerical calculations.

Downloaded 04 Mar 2004 to 129.82.140.198. Redistribution subject to AIP license or copyright, see http://jap.aip.org/jap/copyright.jsp